

---

# Structured Agent Distillation for Large Language Model

---

Jun Liu<sup>1,2</sup> Zhenglun Kong<sup>3</sup> Peiyang Dong<sup>4</sup> Changdi Yang<sup>2</sup> Tianqi Li<sup>1</sup> Hao Tang<sup>5</sup>  
 Geng Yuan<sup>6</sup> Wei Niu<sup>6</sup> Wenbin Zhang<sup>7</sup> Pu Zhao<sup>2</sup> Xue Lin<sup>2</sup> Dong Huang<sup>1</sup> Yanzhi Wang<sup>2</sup>

<sup>1</sup> Carnegie Mellon University <sup>2</sup> Northeastern University <sup>3</sup> Harvard University  
<sup>4</sup> MIT <sup>5</sup> Peking University <sup>6</sup> University of Georgia <sup>7</sup> Florida International University

## Abstract

Large language models (LLMs) exhibit strong capabilities as decision-making agents by interleaving reasoning and actions, as seen in ReAct-style frameworks. Yet, their practical deployment is constrained by high inference costs and large model sizes. We propose **Structured Agent Distillation**, a framework that compresses large *LLM-based general agents* into smaller student models while preserving both reasoning fidelity and action consistency. Unlike standard token-level distillation, our method segments trajectories into [REASON] and [ACT] spans, applying segment-specific losses to align each component with the teacher’s behavior. This structure-aware supervision enables compact agents to better replicate the teacher’s decision process. Experiments on ALFWorld, HotPotQA-ReAct, and WebShop show that our approach consistently outperforms token-level and imitation learning baselines, achieving significant compression with minimal performance drop. Scaling and ablation results further highlight the importance of span-level alignment for efficient and deployable agents.

## 1 Introduction

Large language models (LLMs) have recently been extended beyond language modeling into decision-making roles, giving rise to *LLM-based general agents*—systems that solve complex tasks by interleaving multi-step reasoning and tool-augmented actions. Frameworks like ReAct [1], Toolformer [2], and WebGPT [3] demonstrate that LLMs can operate through structured *reasoning-action trajectories*—sequences alternating between deliberation and execution to complete tasks such as planning, web navigation, and multi-hop question answering. Chain-of-thought (CoT) prompting [4, 5] encourages models to decompose complex tasks into intermediate reasoning steps before acting, reinforcing the need to preserve reasoning-action structure during training.

Despite their effectiveness, LLM-based general agents remain costly to deploy due to model size and inference overhead. To address this, recent work distills large agents into smaller student models. However, most approaches rely on *token-level supervision* [6, 7, 8, 9, 10, 11, 12], which treats the agent trajectory as a flat token sequence and aligns predictions step by step—ignoring its structured composition of reasoning and action.

**Limitations of Token-Level Distillation.** This paradigm fails to capture the *structural nature* of agent behavior: (i) it overlooks long-range dependencies between reasoning and action [13]; (ii) it lacks span-level supervision, blurring the distinction between planning and execution; (iii) it causes semantic drift during rollouts, degrading coherence and task success.

**Our Approach: Structured Agent Distillation.** We propose a structure-aware compression framework that explicitly models the compositional structure of agent behavior. Our method segments each trajectory into [REASON] and [ACT] spans and supervises them with span-specific objectives. By

Table 1: Comparison between LLMs and LLM-based General Agents in terms of token efficiency

Dimension	LLMs	LLM-based General Agents
Application	Static, single-turn tasks (QA, etc.)	Multi-turn interactive tasks (e.g., WebNav)
Objective	Minimize FLOPs in generation	Mini token budget across reasoning + action
Token Source	Fixed input tokens per prompt	Dynamic tokens in reasoning-action steps
Latency Target	Single-step inference efficiency	End-to-end efficiency over agent steps
Output Format	Final text sequence	Task trajectory (reasoning steps + actions)

applying segment-aware masking and reasoning–action alignment, our approach preserves both the rationale and the resulting decision—enabling more faithful and coherent student agents.

### Contributions.

- We introduce a *structured agent distillation framework* that segments teacher trajectories into reasoning and action spans, and applies span-specific supervision via binary token masks—enabling fine-grained alignment beyond token-level imitation.
- We validate our approach on ALFWorld, HotPotQA-ReAct, and WebShop, achieving consistent gains in task success, planning efficiency, and chain-of-thought (CoT) alignment over strong token-level baselines.
- We conduct comprehensive scaling and ablation studies, demonstrating that segment-level supervision is critical for training compact and robust student agents.

## 2 Motivation

### 2.1 Why Token-Level Distillation Falls Short

*LLMs vs. General Agents.* While LLMs focus on single-turn generation, LLM-based general agents operate in interactive settings where structured reasoning and action unfold over multiple steps. Token efficiency in agents must therefore consider trajectory-level [14, 15] latency and semantic role differentiation. Table 1 summarizes the key distinctions between the two paradigms.

This structured nature of agent trajectories poses unique challenges for compression and acceleration. In particular, existing methods such as token-level distillation [6], originally designed for next-token prediction, fail to capture the hierarchical nature of agent behavior.

Token-level distillation supervises the student at each decoding step using cross-entropy [16] or KL divergence [17] between teacher and student outputs. While this is effective for language modeling, it fails to account for the structured nature of agent trajectories—specifically the distinction between intermediate reasoning and final action execution.

Critically, *token-level methods lack structural awareness*, treating all tokens equally without distinguishing their functional roles in the agent trajectory. In practice, trajectories often alternate between internal reasoning steps and external actions—two semantically distinct spans that require different forms of supervision.

As a result, the student learns to match surface-level actions while ignoring the underlying rationale, often skipping key planning steps required to complete the task.

### 2.2 Motivation: Toward Structured Agent Distillation

We propose **Structured Agent Distillation (SAD)**, which segments trajectories into [REASON] and [ACT] spans and applies span-specific supervision to improve structural imitation. A curriculum mechanism further enhances stability by ordering training examples by complexity.

Table 2 summarizes representative LLM-based agent frameworks in terms of four dimensions: external tool usage, reasoning-action alignment, segment-aware supervision, and curriculum-guided training. While prior methods such as ReAct and Voyager support structured reasoning and tool use, they lack segment-level supervision and curriculum scheduling. In contrast, our **Structured Agent Distillation** framework uniquely supports all four dimensions, enabling more faithful and efficient agent compression.

Table 2: Comparison of LLM agent training frameworks. Only our method supports all four dimensions of structured agent distillation. **Tool**: supports external API calls or tool use; **Reasoning-Action** alignment: aligns structured spans (e.g., [REASON], [ACT]); **Segment-aware** supervision: applies supervision across full reasoning-action sequences; **Curriculum**-guided training [18]: uses trajectory difficulty for progressive training.

Framework	Tool	Reasoning-Action	Segm-aware supervision	Curriculum
Token-Level KD [6]	✗	✗	✗	✗
ReAct [1]	✓	✓	✗	✗
Toolformer [2]	✓	✗	✗	✗
Voyager [19]	✓	✓	✗	✗
<b>SAD (Ours)</b>	✓	✓	✓	✓

### 3 Structured Agent Distillation Framework

**Structured Agent Distillation** addresses this by segmenting teacher trajectories into reasoning (Thought) and interaction (Action/Observation) spans, each supervised independently to promote phase-specific alignment.

As shown in Figure 1, The teacher agent, given an initial observation and sampled task, produces a reasoning trajectory and corresponding action. These [REASON] and [ACT] components are extracted into a trajectory  $\tau = (\text{reason}, \text{action})$  used for curriculum sampling.

The student agent learns from this trajectory  $\tau$  via two objectives: (1) *CoT-Policy Alignment Loss*  $\mathcal{L}_{\text{CoT}}$  aligns the reasoning steps, and (2) *Action Consistency Loss*  $\mathcal{L}_{\text{Act}}$  aligns the final action decision. The overall objective is  $\mathcal{L}_{\text{Traj}} = \mathcal{L}_{\text{CoT}} + \mathcal{L}_{\text{Act}}$ .

For a comprehensive analysis, please refer to the Appendix A.

#### 3.1 Problem Formulation

We aim to distill high-capacity ReAct-style teacher agents into smaller student models while preserving structured decision-making behavior. Each teacher’s trajectory is a sequence of interleaved reasoning and action components:

$$\tau = [(r_1, r_2, \dots, r_k), (a_1, a_2, \dots, a_m)], \quad (1)$$

where  $r_i \in \mathcal{R}$  are reasoning tokens (e.g., CoT steps), and  $a_j \in \mathcal{A}$  are action tokens (e.g., tool calls, answers).

Given a teacher policy  $\pi_T(\tau)$ , the goal is to train a compact student policy  $\pi_\theta(\tau)$  such that:

$$\pi_\theta(\tau) \approx \pi_T(\tau), \quad (2)$$

preserving both semantic reasoning and execution structure beyond token-level matching.

To enable sequence-to-sequence modeling, we linearize each trajectory into a flattened form with segment markers:

$$\tau' = [\text{REASON}] r_1 \dots r_k [\text{ACT}] a_1 \dots a_m. \quad (3)$$

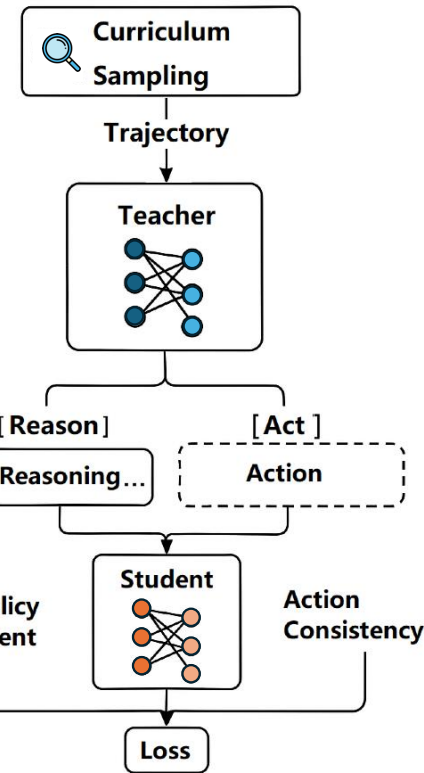


Figure 1: Structured Agent Distillation framework.

We tokenize this as  $x = \text{Tokenize}(\tau') = (x_1, x_2, \dots, x_n)$ , and assign each token  $x_t$  a segment label  $s_t \in \{\text{Reason}, \text{Action}\}$ , indicating its span. These labels are used to compute segment-aware losses during training.

### 3.2 Trajectory Segmentation

Given a teacher-generated trajectory  $\tau$ , we decompose it into two disjoint spans:

$$\tau = (\tau^{(r)}, \tau^{(a)}),$$

where  $\tau^{(r)}$  denotes the reasoning span and  $\tau^{(a)}$  denotes the action span. This segmentation is performed via lightweight rule-based parsing based on prompt templates consistent across tasks (see Appendix D). The segmented trajectory is then tokenized into a sequence  $x = (x_1, x_2, \dots, x_T)$ .

### 3.3 Segment-Aware Supervision via Token Masks

To enable structured supervision in **Structured Agent Distillation**, we construct two binary token-level masks over the tokenized teacher trajectory  $x = (x_1, x_2, \dots, x_T)$ :

- **Reasoning mask**  $m_r(t) \in \{0, 1\}$ :

$$m_r(t) = \begin{cases} 1 & \text{if token } x_t \text{ belongs to a reasoning span,} \\ 0 & \text{otherwise.} \end{cases}$$

- **Action mask**  $m_a(t) \in \{0, 1\}$ :

$$m_a(t) = \begin{cases} 1 & \text{if token } x_t \text{ belongs to an action span,} \\ 0 & \text{otherwise.} \end{cases}$$

Each token belongs to at most one span, so we enforce:

$$m_r(t) + m_a(t) \leq 1, \quad \forall t \in [1, T].$$

This constraint ensures that each token is assigned to at most one functional span, avoiding supervision overlap between reasoning and action phases. These segment-aware masks allow us to decompose the distillation loss and apply span-specific supervision. Mask construction details and validation procedures are provided in Appendix D and F.

### 3.4 Structured Agent Distillation Objectives

To supervise student agents under **Structured Agent Distillation**, we decompose each teacher trajectory  $\tau$  into a reasoning span  $\tau^{(r)}$  and an action span  $\tau^{(a)}$  (see Appendix D for segmentation rules). The full trajectory is tokenized into  $x = (x_1, \dots, x_T)$  and aligned with binary token masks  $m_r(t)$  and  $m_a(t)$ , which indicate whether token  $x_t$  belongs to the reasoning or action span, respectively. These **segment-aware masks** enable selective supervision over structurally distinct parts of the trajectory.

Given these segment-aware masks, the student policy  $\pi_\theta$  is supervised through two loss terms:

**(1) CoT-Policy Alignment Loss.** We align the student’s predicted distribution  $p_S(x_t)$  with the teacher distribution  $p_T(x_t)$  for reasoning tokens using KL divergence:

$$\mathcal{L}_{\text{CoT}} = \sum_{t=1}^T m_r(t) \cdot \text{KL}(p_T(x_t) \| p_S(x_t)). \quad (4)$$

**(2) Action Consistency Loss.** For action tokens, we similarly minimize KL divergence:

$$\mathcal{L}_{\text{Act}} = \sum_{t=1}^T m_a(t) \cdot \text{KL}(p_T(x_t) \| p_S(x_t)). \quad (5)$$

**Final Objective.** The total structured loss aggregates these terms:

$$\mathcal{L}_{\text{total}} = \lambda_r \cdot \mathcal{L}_{\text{CoT}} + \lambda_a \cdot \mathcal{L}_{\text{Act}}, \quad (6)$$

where  $\lambda_r$  and  $\lambda_a$  are scalar weights balancing the two objectives. We set  $\lambda_r = \lambda_a = 1.0$  to equally weight reasoning and action supervision in the final loss.

**Semantic Decoupling.** While the overall loss is additive in form, our supervision is fundamentally different from flat token-level imitation. We explicitly decompose the learning signal into structurally disjoint spans—[REASON] and [ACT]—and apply segment-specific losses to each, preserving the semantics of multi-phase agent behavior.

**CoT-Policy Alignment Loss** ( $\mathcal{L}_{\text{CoT}}$ ) supervises predictions within the reasoning span, promoting coherent multi-step inference aligned with teacher thought patterns. The reasoning-action example below highlights span-specific KL penalties.

**Action Consistency Loss** ( $\mathcal{L}_{\text{Act}}$ ) applies only to the action span, enforcing accurate replication of grounded decisions.

Each token is assigned to exactly one functional span using binary masks  $\{m_r(t), m_a(t)\}$ , which gate gradient flow. This masking is not heuristic—it enforces *semantic separation* during training, ensuring that the student independently learns high-level reasoning and low-level execution.

Unlike token-level KL with soft targets, our structure-aware formulation avoids loss interference across phases, better modeling causal dependencies (e.g., reason  $\rightarrow$  act). Ablation results confirm that removing either component harms performance, underscoring their complementary roles in agent compositionality.

This separation ensures that students do not overfit to output correctness alone, but also learn to emulate coherent decision logic.

**Example.** Reasoning-action trajectory from the teacher and the corresponding imitation by the student:

**Instruction:** "Find the tray"

**Teacher:** [REASON] "I will first look on the table to check for a tray..."  $\rightarrow$  [ACT] search[tray]

**Student:** [REASON] "Maybe it's on the shelf, I should check there."  $\rightarrow$  [ACT] search[tray]

Although the student executes the correct action (search[tray]), its reasoning deviates from the teacher's thought process. The **CoT-Policy Alignment Loss** penalizes semantic deviations within the reasoning span ([REASON]) by computing KL divergence between the teacher and student token distributions. When the student generates thought tokens inconsistent with the teacher's, the KL divergence increases, producing gradients that push the student toward reproducing the teacher's multi-step reasoning trace. In contrast, the **Action Consistency Loss** rewards correct predictions in the [ACT] span, allowing action alignment even when reasoning differs.

### 3.5 Curriculum Sampling in Structured Distillation

To further enhance learning efficiency and stability, we employ curriculum learning [20, 21] based on a trajectory complexity score:

$$C(\tau) = \alpha \cdot \text{len}(r_{1:k}) + \beta \cdot \text{len}(a_{1:m}) + \gamma \cdot \text{entropy}(\pi_T(\tau)), \quad (7)$$

where  $\text{len}(r_{1:k})$  and  $\text{len}(a_{1:m})$  denote the lengths of the reasoning and action segments, respectively, and  $\text{entropy}(\pi_T(\tau))$  reflects teacher uncertainty. The weights  $\alpha, \beta, \gamma$  balance their relative contributions. During training, trajectories are sorted by  $C(\tau)$ , allowing the model to start with simpler examples and gradually progress to more complex ones.

### 3.6 Training Algorithm

Algorithm 1 outlines our structured agent distillation process. The student policy  $\pi_\theta$  learns to imitate the teacher  $\pi_T$  across reasoning stages, guided by a curriculum scheduler  $\mathcal{C}$  that samples increasingly complex trajectories. Each trajectory is tokenized into reasoning and action spans, and the student predicts tokens autoregressively. The objective aggregates reasoning, action imitation losses, and gradients are backpropagated to update  $\theta$ .

Table 3: Unified comparison of task success ( $\uparrow$ ), reasoning length ( $\downarrow$ ), CoT match ( $\uparrow$ ), and latency ( $\downarrow$ ) across ALFWorld, WebShop, and HotPotQA. The teacher is a GPT-2-1.5B ReAct-style agent. Students trained via **Structured Agent Distillation** consistently outperform token-level baselines [9].

Method	Task Success $\uparrow$			Reasoning Length $\downarrow$			CoT Match Rate $\uparrow$			Episode Latency $\downarrow$		
	ALF	Web	Hot	ALF	Web	Hot	ALF	Web	Hot	ALF	Web	Hot
Teacher(GPT)	71.2	68.7	78.5	8.2	11.5	10.8	100.0	100.0	100.0	5.8	7.4	6.2
Token-120M	39.4	36.7	48.3	12.4	15.7	14.8	59.3	55.1	65.7	9.1	10.7	8.9
Ours (120M)	<b>43.7</b>	<b>41.2</b>	<b>52.8</b>	<b>11.2</b>	<b>14.6</b>	<b>13.8</b>	<b>62.3</b>	<b>58.7</b>	<b>66.2</b>	<b>8.2</b>	<b>9.5</b>	<b>7.8</b>
Toke-340M	52.1	49.8	61.5	10.6	14.1	13.0	68.1	62.4	70.5	7.8	9.4	7.9
Ours (340M)	<b>56.3</b>	<b>54.7</b>	<b>65.5</b>	<b>9.8</b>	<b>13.1</b>	<b>12.2</b>	<b>71.5</b>	<b>66.9</b>	<b>74.0</b>	<b>7.1</b>	<b>8.7</b>	<b>7.0</b>
Token-760M	60.2	57.0	69.1	9.5	13.2	12.0	74.0	69.3	76.4	7.0	8.6	7.2
Ours (760M)	<b>64.8</b>	<b>61.5</b>	<b>73.1</b>	<b>8.9</b>	<b>12.4</b>	<b>11.7</b>	<b>77.9</b>	<b>73.1</b>	<b>80.4</b>	<b>6.4</b>	<b>8.1</b>	<b>6.6</b>

---

**Algorithm 1** Structured Agent Distillation

---

- 1: Initialize teacher policy  $\pi_T$ , student policy  $\pi_\theta$ , and curriculum scheduler  $\mathcal{C}$
- 2: **for** epoch = 1 to E **do**
- 3:   Sample trajectory  $\tau \sim \mathcal{C}$
- 4:   Segment into  $\tau^{(r)}, \tau^{(a)}$  and tokenize  $x_{1:T}$
- 5:   Compute segment masks  $m_r, m_a$
- 6:   Perform forward pass  $\hat{x} = \pi_\theta(x)$
- 7:   Compute losses  $\mathcal{L}_{\text{cot}}, \mathcal{L}_{\text{act}}$
- 8:   Backpropagate  $\mathcal{L}_{\text{total}}$  and Update  $\theta \leftarrow \theta - \nabla \mathcal{L}_{\text{total}}$
- 9: **end for**

---

## 4 Experiments

### 4.1 Experimental Setups

**Agent Environments.** We evaluate our framework on three agent environments: **(i)** ALFWorld [22] for embodied instruction following, **(ii)** WebShop [23] for web-based tool planning, and **(iii)** HotPotQA-ReAct [1] for multi-hop QA with reasoning traces. Task-specific details are in Appendix B.

**Models.** We apply **Structured Agent Distillation** to compress ReAct-style GPT-2-1.5B teacher trajectories into student models of 120M, 340M, and 760M (GPT-2); OPT-13B into OPT students (1.3B, 2.7B, 6.7B); and LLaMA-13B into LLaMA-7B.

Trajectories are generated offline via low-temperature ReAct prompts, segmented into reasoning and action spans (Appendix D), and used to train students with segment-aware losses.

**Metrics.** We evaluate student agents on: **(i)** task success rate [24], **(ii)** average reasoning length (efficiency), **(iii)** CoT match rate (consistency), and **(iv)** latency (reasoning + action steps). Metric definitions are in Appendix C.

**Baselines.** Our goal is not to exhaustively benchmark all existing distillation methods, but rather to evaluate how span-level alignment improves student agent fidelity under comparable conditions. We compare against token-level baselines, primarily using MiniLLM [9]—a state-of-the-art student model distilled from GPT-2 via token-level imitation, which minimizes the KL divergence between student and teacher outputs at every decoding step.

### 4.2 Experimental Results and Analysis

We evaluate student agent performance across three benchmarks—ALFWorld, WebShop, and HotPotQA-ReAct—comparing our proposed **Structured Agent Distillation** with the baseline. We report results across three evaluation metrics: task success rate, reasoning efficiency, and CoT consistency (Table 3).

Table 4: Unified comparison of task success ( $\uparrow$ ), reasoning length ( $\downarrow$ ), CoT match ( $\uparrow$ ), and latency ( $\downarrow$ ) across ALFWorld, WebShop, and HotPotQA. The teachers are OPT-13B and LLaMA-13B ReAct-style agents. Students trained via **Structured Agent Distillation** consistently outperform token-level baselines [9].

Model	Task Success $\uparrow$			Reasoning Length $\downarrow$			CoT Match $\uparrow$			Latency $\downarrow$		
	ALF	Web	Hot	ALF	Web	Hot	ALF	Web	Hot	ALF	Web	Hot
Teacher (OP13B)	76.5	73.2	82.7	38.2	35.9	40.7	100.0	100.0	100.0	6.5	5.9	4.8
Token-OPT-1.3B	47.8	43.2	54.1	45.7	41.8	48.5	61.5	57.9	69.8	7.8	7.1	6.0
Ours (OPT-1.3B)	<b>52.3</b>	<b>48.7</b>	<b>58.5</b>	<b>41.2</b>	<b>38.0</b>	<b>43.6</b>	<b>67.2</b>	<b>63.8</b>	<b>74.4</b>	<b>7.0</b>	<b>6.4</b>	<b>5.3</b>
Token-OPT-2.7B	55.6	51.0	62.9	42.5	39.0	45.2	67.3	62.7	75.5	7.2	6.6	5.6
Ours (OPT-2.7B)	<b>59.2</b>	<b>56.4</b>	<b>67.0</b>	<b>39.4</b>	<b>36.2</b>	<b>41.7</b>	<b>71.6</b>	<b>67.9</b>	<b>79.8</b>	<b>6.7</b>	<b>6.1</b>	<b>5.0</b>
Token-OPT-6.7B	62.8	58.6	69.7	40.8	37.2	42.9	72.2	67.9	80.2	6.8	6.2	5.3
Ours (OPT-6.7B)	<b>67.1</b>	<b>63.8</b>	<b>73.9</b>	<b>38.0</b>	<b>35.1</b>	<b>40.2</b>	<b>76.4</b>	<b>72.5</b>	<b>84.0</b>	<b>6.5</b>	<b>5.9</b>	<b>4.9</b>
Teacher (LLaMA13B)	75.3	71.8	81.0	37.5	34.8	39.9	100.0	100.0	100.0	6.4	5.8	4.7
Toke-LLaMA-7B	64.2	59.3	71.5	41.1	37.5	43.2	73.0	68.3	81.2	6.7	6.1	5.2
Ours (LLaMA-7B)	<b>68.0</b>	<b>64.1</b>	<b>75.2</b>	<b>38.2</b>	<b>34.9</b>	<b>39.8</b>	<b>77.2</b>	<b>72.9</b>	<b>84.7</b>	<b>6.4</b>	<b>5.8</b>	<b>4.8</b>

**Task Success Rate.** As shown in Table 3, **Structured Agent Distillation** consistently outperforms token-level MiniLLM baselines across all student sizes, with especially notable gains at 120M (+4.3%), confirming the effectiveness of trajectory-level supervision over token imitation.

**Reasoning Efficiency.** Table 3 shows that students trained via **Structured Agent Distillation** generate shorter reasoning spans.

**CoT Consistency.** As shown in Table 3, our method achieves higher CoT match rates across all settings, demonstrating stronger structural alignment with teacher reasoning.

**Latency.** Following prior work [1, 15], we measure the average number of reasoning and action steps per episode. As shown in Table 3, **segment-aware** students consistently exhibit shorter execution traces. Latency is measured in reasoning/action steps rather than wall-clock time, and lower values indicate more concise and efficient decision-making.

**Segment Mask Validation.** Figure 7 (Appendix F.2) confirms that token-level masks align accurately with reasoning/action spans across environments.

**Span Statistics.** As shown in Figure 8, reasoning spans are longer and more variable, while action spans are shorter—justifying span-specific supervision.

**Summary.** Our method outperforms token-level distillation across all benchmarks (Table 4), yielding more accurate and faithful student agents.

## 5 Scaling Analysis

We evaluate how **Structured Agent Distillation** scales by transferring GPT-2-1.5B teacher trajectories into student models with 120M, 340M, and 760M parameters, compared against corresponding MiniLLM-OPT-GPT2 baselines.

Figure 2 summarizes four metrics—task success rate, reasoning efficiency (avg. reasoning length), CoT match rate, and episode latency—on ALFWorld, WebShop, and HotPotQA-ReAct.

**Task Success.** Success rates improve with model size (top-left), with students trained via **Structured Agent Distillation** consistently outperforming token-level baselines. At 760M, performance closely approaches the teacher.

**Reasoning Efficiency.** Students trained via **Structured Agent Distillation** produce shorter, more efficient reasoning traces (top-right), especially at larger scales.

**CoT Match.** Students distilled with our method better recover the teacher’s reasoning structure (bottom-left), with consistently higher CoT match rates.

**Latency.** Structured supervision yields lower episode latency (bottom-right), reducing decision steps and accelerating task completion.

**Summary.** **Structured Agent Distillation** scales effectively with student capacity, enhancing task success, planning efficiency, and structural reasoning alignment. Improvements are most pronounced at smaller scales (e.g., 120M, 340M), where it mitigates the performance degradation commonly

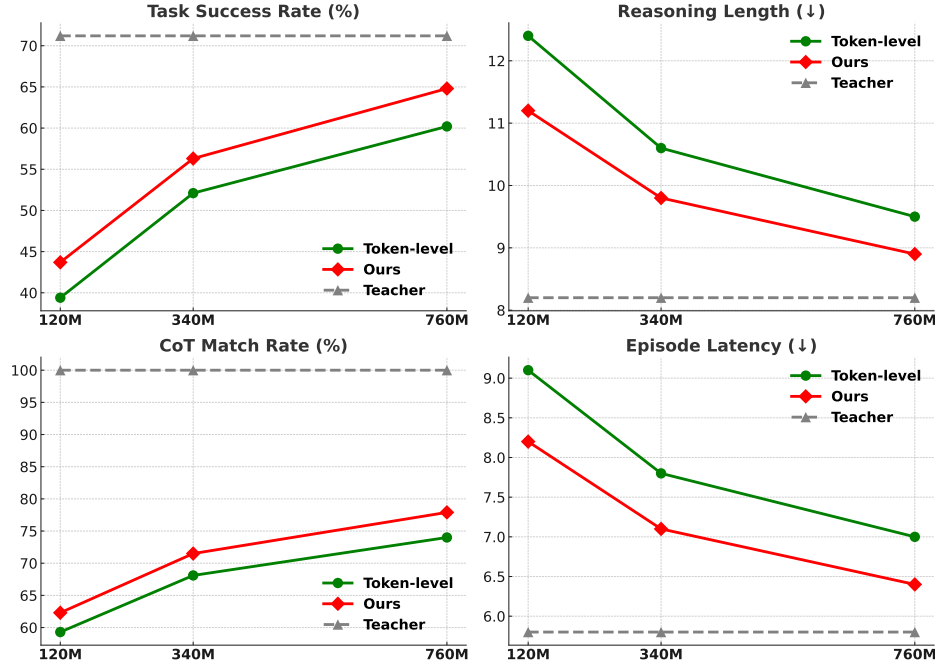


Figure 2: Scaling behavior of student agents across model sizes. **Top-Left:** Task Success Rate (%). **Top-Right:** Reasoning Length (tokens). **Bottom-Left:** Chain-of-Thought (CoT) Match Rate (%). **Bottom-Right:** Latency (steps per episode). **Structured Agent Distillation** consistently outperforms MiniLLM-OPT baselines and better approaches teacher performance as model capacity increases.

Table 5: Ablation study on ALFWorld using a 340M-parameter student model. Each variant controls whether reasoning, action supervision, and explicit span segmentation are enabled. We report task success rate, CoT match rate, and episode latency(steps).

Method	Reason	Action	Segm	Succ (%) ↑	CoT (%) ↑	Steps ↓
Full Segment-Aware (Ours)	✓	✓	✓	<b>56.3</b>	<b>71.5</b>	<b>7.1</b>
Only Reasoning Supervision	✓	✗	✓	52.7	69.2	7.4
Only Action Supervision	✗	✓	✓	49.5	61.8	7.8
No Span Segmentation	✓	✓	✗	48.2	60.4	8.1
Random Span Masking	✓	✓	~ (random)	45.9	57.7	8.4

observed with token-level imitation. Additional scaling results for OPT and LLaMA models are presented in Appendix G.

## 6 Ablation Studies

We conduct ablation studies to understand the contribution of each component in our **Structured Agent Distillation** framework. Specifically, we analyze the roles of reasoning supervision, action supervision, and span segmentation.

Table 5 confirms that each supervision component plays a critical role:

**Removing reasoning supervision** ( $\mathcal{L}_{\text{CoT}}$ ) significantly degrades CoT match and increases latency, indicating reduced planning coherence.

**Removing action supervision** ( $\mathcal{L}_{\text{Act}}$ ) lowers task success and execution fidelity, showing the importance of behavior alignment.

**Disabling span segmentation** (flat token-level loss) causes uniform degradation across all metrics, suggesting that structural decomposition is essential.

**Random span masking** further harms performance, highlighting the need for accurate, semantically meaningful segmentation.

These results demonstrate that our method goes beyond masked token-level imitation—segment-aware supervision captures structurally distinct signals crucial for reasoning-action alignment.

## 7 Discussion

**Semantic Decoupling Matters.** Our results show that simply applying token-level imitation—even with large-scale training—fails to preserve the structure of reasoning-action workflows. By explicitly segmenting trajectories and supervising each span separately, **Structured Agent Distillation** enables student models to independently learn symbolic reasoning and grounded execution behaviors. This semantic decoupling proves essential, especially under limited capacity.

**Loss Design and Supervision.** Although our total loss aggregates  $\mathcal{L}_{\text{CoT}}$  and  $\mathcal{L}_{\text{Act}}$ , they are not functionally redundant. As shown in ablation studies, removing either term leads to substantial drops in performance across CoT alignment, task success, and planning efficiency. This confirms that span-level supervision provides complementary guidance that token-level KL losses alone cannot capture.

**Robustness of Rule-Based Segmentation.** Our segmentation pipeline relies on task-specific patterns to extract [REASON] and [ACT] spans. While simple, this rule-based approach is highly reliable across benchmarks and avoids the cost of manual annotation. Empirically, segmentation accuracy is sufficient to yield clear improvements in student performance.

**Limitations.** Our current framework is designed for text-only agents operating under ReAct-style assumptions. It does not yet model multimodal spans (e.g., vision-language), nor does it account for agent memory or external feedback loops.

**Future Work.** We aim to extend span-aware supervision to multimodel agents, and explore alignment for more complex structures, such as hierarchical subgoals or latent plans. We plan to use diffusion models [25] to generate small samples [26, 27, 28] for multimodal agent research in healthcare [29, 30, 31, 32]. These samples will be combined with large language models (LLMs) for downstream tasks such as 3D reconstruction [33, 34, 35]. In parallel, we will benchmark recent compression techniques [36, 37, 38, 39, 40, 41, 42, 43] to support efficient deployment on embedded devices [44, 45, 37, 42, 46].

## 8 Related Work

### LLM Agents.

LLM agents unify reasoning and action. ReAct [1] interleaves language and actions. Toolformer [2] self-supervises API calls, while WebGPT [3] reasons via web browsing. AutoGPT [47] chains subtasks autonomously. AgentBench [24], ReWoo [48], and HuggingGPT [49] explore modularity and tool use. CAMEL [50], ChatDev [51], AutoGen [52], CrewAI [53], ToolBench [54], and LangChain [55] focus on multi-agent collaboration and LLM orchestration. GITM [56] integrates LLMs with memory and knowledge to build generally capable agents. Although these agents show strong reasoning-action abilities, their trajectories remain challenging to compress and generalize.

**Distillation and Fine-Tuning.** Token-level distillation [6, 7, 8, 9, 10, 11, 12] compresses LLMs via soft target alignment and teacher-guided training. Recent work improves multi-granular supervision [9], cross-modal transfer [57], and compact pretraining [58]. However, these methods target static text generation, not structured reasoning-action trajectories.

**Trajectory Modeling and Behavioral Cloning.** Recent work in sequence-level imitation [5, 59, 60, 61, 62, 63, 64], behavior cloning [65, 66, 67, 68, 69, 70], and diffusion planning [71] emphasizes temporal coherence in agent behavior. SpanBERT [72] masks contiguous spans instead of individual tokens. ConvBERT [73] uses span-based convolutions instead of attention heads. LLM agents require structured objectives to model reasoning and action jointly—captured by our **Structured Agent Distillation** framework.

## 9 Conclusion

We propose **Structured Agent Distillation**, a structured compression framework that segments teacher trajectories into reasoning and action spans, enabling student agents to better mimic high-level reasoning and low-level execution beyond shallow token-level imitation.

Experiments on ALFWorld, WebShop, and HotPotQA-ReAct demonstrate consistent gains in task success, reasoning efficiency, and CoT consistency over token-level baselines. Scaling and ablation studies further highlight the value of structured supervision under limited capacity.

Our results underscore the importance of preserving agent trajectory structure for training lightweight, deployable agents, paving the way for future work in structured knowledge transfer and real-world decision-making.

## References

- [1] Shunyu Yao, Jeffrey Zhao, Dian Yu, Nan Du, Izhak Shafran, Karthik Narasimhan, and Yuan Cao. React: Synergizing reasoning and acting in language models. In *International Conference on Learning Representations (ICLR)*, 2023.
- [2] Timo Schick, Jane Dwivedi-Yu, Roberto Dessì, Roberta Raileanu, Maria Lomeli, Eric Hambro, Luke Zettlemoyer, Nicola Cancedda, and Thomas Scialom. Toolformer: Language models can teach themselves to use tools. *Advances in Neural Information Processing Systems*, 36:68539–68551, 2023.
- [3] Reiichiro Nakano, Jacob Hilton, Suchir Balaji, Jeff Wu, Long Ouyang, Christina Kim, Christopher Hesse, Shantanu Jain, Vineet Kosaraju, William Saunders, et al. Webgpt: Browser-assisted question-answering with human feedback. *arXiv preprint arXiv:2112.09332*, 2021.
- [4] Jason Wei, Xuezhi Wang, Dale Schuurmans, Maarten Bosma, Fei Xia, Ed Chi, Quoc V Le, Denny Zhou, et al. Chain-of-thought prompting elicits reasoning in large language models. *Advances in neural information processing systems*, 35:24824–24837, 2022.
- [5] Xuezhi Wang, Jason Wei, Dale Schuurmans, Quoc Le, Ed Chi, Sharan Narang, Aakanksha Chowdhery, and Denny Zhou. Self-consistency improves chain of thought reasoning in language models. *arXiv preprint arXiv:2203.11171*, 2022.
- [6] Geoffrey Hinton, Oriol Vinyals, and Jeff Dean. Distilling the knowledge in a neural network. *arXiv preprint arXiv:1503.02531*, 2015.
- [7] Iulia Turc, Ming-Wei Chang, Kenton Lee, and Kristina Toutanova. Well-read students learn better: The impact of student initialization on knowledge distillation. *arXiv preprint arXiv:1908.08962*, 2019.
- [8] Ronen Eldan and Yuanzhi Li. Tinystories: How small can language models be and still speak coherent english? *arXiv preprint arXiv:2305.07759*, 2023.
- [9] Yuxian Gu, Li Dong, Furu Wei, and Minlie Huang. MiniLLM: Knowledge distillation of large language models. In *The Twelfth International Conference on Learning Representations*, 2024.
- [10] Benjamin Minixhofer, Edoardo Maria Ponti, and Ivan Vulić. Cross-tokenizer distillation via approximate likelihood matching. *arXiv preprint arXiv:2503.20083*, 2025.
- [11] Xiao Cui, Mo Zhu, Yulei Qin, Liang Xie, Wengang Zhou, and Houqiang Li. Multi-level optimal transport for universal cross-tokenizer knowledge distillation on language models. In *Proceedings of the AAAI Conference on Artificial Intelligence*, volume 39, pages 23724–23732, 2025.
- [12] Shuoxi Zhang, Hanpeng Liu, and Kun He. Knowledge distillation via token-level relationship graph based on the big data technologies. *Big Data Research*, 36:100438, 2024.
- [13] Lianmin Zheng, Liangsheng Yin, Zhiqiang Xie, Chuyue Livia Sun, Jeff Huang, Cody Hao Yu, Shiyi Cao, Christos Kozyrakis, Ion Stoica, Joseph E Gonzalez, et al. Sqlang: Efficient execution of structured language model programs. *Advances in Neural Information Processing Systems*, 37:62557–62583, 2024.
- [14] Scott Reed, Konrad Zolna, Emilio Parisotto, Sergio Gómez Colmenarejo, Alexander Novikov, Gabriel Barth-maron, Mai Giménez, Yury Sulsky, Jackie Kay, Jost Tobias Springenberg, et al. A generalist agent. *Transactions on Machine Learning Research*, 2022.
- [15] Noah Shinn, Federico Cassano, Ashwin Gopinath, Karthik Narasimhan, and Shunyu Yao. Reflexion: Language agents with verbal reinforcement learning. *Advances in Neural Information Processing Systems*, 36:8634–8652, 2023.

- [16] Thomas M Cover. *Elements of information theory*. John Wiley & Sons, 1999.
- [17] Solomon Kullback and Richard A Leibler. On information and sufficiency. *The Annals of Mathematical Statistics*, 22(1):79–86, 1951.
- [18] M Kumar, Benjamin Packer, and Daphne Koller. Self-paced learning for latent variable models. *Advances in neural information processing systems*, 23, 2010.
- [19] Guanzhi Wang, Yuqi Xie, Yunfan Jiang, Ajay Mandlekar, Chaowei Xiao, Yuke Zhu, Linxi Fan, and Anima Anandkumar. Voyager: An open-ended embodied agent with large language models. *arXiv preprint arXiv:2305.16291*, 2023.
- [20] Yoshua Bengio, Jean Louradour, Ronan Collobert, and Jason Weston. Curriculum learning. In *Proceedings of the 26th Annual International Conference on Machine Learning (ICML 2009)*, pages 41–48. ACM, 2009.
- [21] Sheng Guo, Weilin Huang, Haozhi Zhang, Chenfan Zhuang, Dengke Dong, Matthew R Scott, and Dinglong Huang. Curriculunet: Weakly supervised learning from large-scale web images. In *Proceedings of the European conference on computer vision (ECCV)*, pages 135–150, 2018.
- [22] Mohit Shridhar, Xingdi Yuan, Marc-Alexandre Côté, Yonatan Bisk, Adam Trischler, and Matthew Hausknecht. ALFWorld: Aligning Text and Embodied Environments for Interactive Learning. In *Proceedings of the International Conference on Learning Representations (ICLR)*, 2021.
- [23] Shunyu Yao, Howard Chen, John Yang, and Karthik Narasimhan. Webshop: Towards scalable real-world web interaction with grounded language agents. In *ArXiv*, preprint.
- [24] Xiao Liu, Hao Yu, Hanchen Zhang, Yifan Xu, Xuanyu Lei, Hanyu Lai, Yu Gu, Hangliang Ding, Kaiwen Men, Kejuan Yang, et al. Agentbench: Evaluating llms as agents. *arXiv preprint arXiv:2308.03688*, 2023.
- [25] Zichong Meng, Changdi Yang, Jun Liu, Hao Tang, Pu Zhao, and Yanzhi Wang. Instructgie: Towards generalizable image editing. In *European Conference on Computer Vision*, pages 18–34. Springer, 2024.
- [26] Jun Liu, Geng Yuan, Changdi Yang, Houbing Song, and Liang Luo. An interpretable cnn for the segmentation of the left ventricle in cardiac mri by real-time visualization. *CMES-Computer Modeling in Engineering & Sciences*, 135(2), 2023.
- [27] Jun Liu, Feng Deng, Geng Yuan, Xue Lin, Houbing Song, and Yanzhi Wang. An explainable convolutional neural networks for automatic segmentation of the left ventricle in cardiac mri. In *CECNet*, pages 306–314, 2021.
- [28] Jun Liu, Feng Deng, Geng Yuan, Changdi Yang, Houbing Song, and Liang Luo. An efficient cnn for radiogenomic classification of low-grade gliomas on mri in a small dataset. *Wireless Communications and Mobile Computing*, 2022(1):8856789, 2022.
- [29] Jun Liu, Geng Yuan, Weihao Zeng, Hao Tang, Wenbin Zhang, Xue Lin, XiaoLin Xu, Dong Huang, and Yanzhi Wang. Brain tumor classification on mri in light of molecular markers. *arXiv preprint arXiv:2409.19583*, 2024.
- [30] Sribala Vidyadhari Chinta, Karen Fernandes, Ningxi Cheng, Jordan Fernandez, Shamim Yazdani, Zhipeng Yin, Zichong Wang, Xuyu Wang, Weifeng Xu, Jun Liu, et al. Optimization and improvement of fake news detection using voting technique for societal benefit. In *2023 IEEE International Conference on Data Mining Workshops (ICDMW)*, pages 1565–1574. IEEE, 2023.
- [31] Zichong Wang, Zhipeng Yin, Yuying Zhang, Liping Yang, Tingting Zhang, Niki Pissinou, Yu Cai, Shu Hu, Yun Li, Liang Zhao, et al. Graph fairness via authentic counterfactuals: Tackling structural and causal challenges. *ACM SIGKDD Explorations Newsletter*, 26(2):89–98, 2025.
- [32] Sribala Vidyadhari Chinta, Zichong Wang, Xingyu Zhang, Thang Doan Viet, Ayesha Kashif, Monique Antoinette Smith, and Wenbin Zhang. Ai-driven healthcare: A survey on ensuring fairness and mitigating bias. *arXiv preprint arXiv:2407.19655*, 2024.

- [33] Yutian Lei, Jun Liu, and Dong Huang. Mac: Modality calibration for object detection. *arXiv preprint arXiv:2310.09461*, 2023.
- [34] Haoye Dong, Tiange Xiang, Sravan Chittupalli, Jun Liu, and Dong Huang. Physical-space multi-body mesh detection achieved by local alignment and global dense learning. In *Proceedings of the IEEE/CVF Winter Conference on Applications of Computer Vision*, pages 1267–1276, 2024.
- [35] Haoye Dong, Jun Liu, and Dong Huang. Df-vton: Dense flow guided virtual try-on network. In *ICASSP 2024-2024 IEEE International Conference on Acoustics, Speech and Signal Processing (ICASSP)*, pages 3175–3179. IEEE, 2024.
- [36] Qitao Tan, Sung-En Chang, Rui Xia, Huidong Ji, Chence Yang, Ci Zhang, Jun Liu, Zheng Zhan, Zhou Zou, Yanzhi Wang, et al. Perturbation-efficient zeroth-order optimization for hardware-friendly on-device training. *arXiv preprint arXiv:2504.20314*, 2025.
- [37] Jun Liu, Zhenglun Kong, Pu Zhao, Weihao Zeng, Hao Tang, Xuan Shen, Changdi Yang, Wenbin Zhang, Geng Yuan, Wei Niu, et al. Tsla: A task-specific learning adaptation for semantic segmentation on autonomous vehicles platform. *IEEE Transactions on Computer-Aided Design of Integrated Circuits and Systems*, 2024.
- [38] Jun Liu, Zhenglun Kong, Peiyan Dong, Xuan Shen, Pu Zhao, Hao Tang, Geng Yuan, Wei Niu, Wenbin Zhang, Xue Lin, et al. Rora: Efficient fine-tuning of llm with reliability optimization for rank adaptation. *arXiv preprint arXiv:2501.04315*, 2025.
- [39] Jun Liu, Zhenglun Kong, Pu Zhao, Changdi Yang, Hao Tang, Xuan Shen, Geng Yuan, Wei Niu, Wenbin Zhang, Xue Lin, et al. Toward adaptive large language models structured pruning via hybrid-grained weight importance assessment. *arXiv preprint arXiv:2403.10799*, 2024.
- [40] Sheng Li, Qitao Tan, Yue Dai, Zhenglun Kong, Tianyu Wang, Jun Liu, Ao Li, Ninghao Liu, Yufei Ding, Xulong Tang, et al. Mutual effort for efficiency: A similarity-based token pruning for vision transformers in self-supervised learning. In *The Thirteenth International Conference on Learning Representations*.
- [41] Qitao Tan, Jun Liu, Zheng Zhan, Caiwei Ding, Yanzhi Wang, Jin Lu, and Geng Yuan. Harmony in divergence: Towards fast, accurate, and memory-efficient zeroth-order llm fine-tuning. *arXiv preprint arXiv:2502.03304*, 2025.
- [42] Huidong Ji, Sheng Li, Yue Cao, Chen Ding, Jiawei Xu, Qitao Tan, Jun Liu, Ao Li, Xulong Tang, Lirong Zheng, et al. A computation and energy efficient hardware architecture for ssl acceleration. In *Proceedings of the 30th Asia and South Pacific Design Automation Conference*, pages 23–29, 2025.
- [43] Jun Liu, Zhenglun Kong, Pu Zhao, Changdi Yang, Xuan Shen, Hao Tang, Geng Yuan, Wei Niu, Wenbin Zhang, Xue Lin, et al. Toward adaptive large language models structured pruning via hybrid-grained weight importance assessment. In *Proceedings of the AAAI Conference on Artificial Intelligence*, volume 39, pages 18879–18887, 2025.
- [44] Geng Yuan, Peiyan Dong, Mengshu Sun, Wei Niu, Zhengang Li, Yuxuan Cai, Jun Liu, Weiwen Jiang, Xue Lin, Bin Ren, et al. Work in progress: Mobile or fpga? a comprehensive evaluation on energy efficiency and a unified optimization framework. In *2021 IEEE 27th Real-Time and Embedded Technology and Applications Symposium (RTAS)*, pages 493–496. IEEE, 2021.
- [45] Geng Yuan, Peiyan Dong, Mengshu Sun, Wei Niu, Zhengang Li, Yuxuan Cai, Yanyu Li, Jun Liu, Weiwen Jiang, Xue Lin, et al. Mobile or fpga? a comprehensive evaluation on energy efficiency and a unified optimization framework. *ACM Transactions on Embedded Computing Systems*, 21(5):1–22, 2022.
- [46] Jun Liu, Chao Wu, Geng Yuan, Wei Niu, Wenbin Zhang, and Houbing Herbert Song. A scalable real-time semantic segmentation network for autonomous driving. In *Proceedings of the 2023 Workshop on Advanced Multimedia Computing for Smart Manufacturing and Engineering*, pages 3–12, 2023.

[47] Toran Bruce Richards and Significant Gravitas. AutoGPT: An experimental open-source attempt to make GPT-4 autonomous. <https://github.com/Significant-Gravitas/AutoGPT>, 2023. Accessed: 2025-04-15.

[48] Binfeng Xu, Zhiyuan Peng, Bowen Lei, Subhabrata Mukherjee, Yuchen Liu, and Dongkuan Xu. Rewoo: Decoupling reasoning from observations for efficient augmented language models. *arXiv preprint arXiv:2305.18323*, 2023.

[49] Yongliang Shen, Kaitao Song, Xu Tan, Dongsheng Li, Weiming Lu, and Yueling Zhuang. Hugginggpt: Solving ai tasks with chatgpt and its friends in hugging face. *Advances in Neural Information Processing Systems*, 36:38154–38180, 2023.

[50] Guohao Li, Hasan Abed Al Kader Hammoud, Hani Itani, Dmitrii Khizbulin, and Bernard Ghanem. Camel: Communicative agents for "mind" exploration of large language model society. In *Thirty-seventh Conference on Neural Information Processing Systems*, 2023.

[51] Chen Qian, Wei Liu, Hongzhang Liu, Nuo Chen, Yufan Dang, Jiahao Li, Cheng Yang, Weize Chen, Yusheng Su, Xin Cong, Juyuan Xu, Dahai Li, Zhiyuan Liu, and Maosong Sun. Chatdev: Communicative agents for software development. *arXiv preprint arXiv:2307.07924*, 2023.

[52] Qingyun Wu, Gagan Bansal, Jieyu Zhang, Yiran Wu, Beibin Li, Erkang Zhu, Li Jiang, Xiaoyun Zhang, Shaokun Zhang, Jiale Liu, et al. Autogen: Enabling next-gen llm applications via multi-agent conversation. *arXiv preprint arXiv:2308.08155*, 2023.

[53] CrewAI Inc. CrewAI: Framework for Orchestrating Role-Playing, Autonomous AI Agents. <https://github.com/crewAIInc/crewAI>, 2023. Accessed: 2025-04-15.

[54] Zhicheng Guo, Sijie Cheng, Hao Wang, Shihao Liang, Yujia Qin, Peng Li, Zhiyuan Liu, Maosong Sun, and Yang Liu. Stabletoolbench: Towards stable large-scale benchmarking on tool learning of large language models, 2024.

[55] LangChain Inc. LangChain Documentation. <https://python.langchain.com/>, 2022. Accessed: 2025-04-15.

[56] Xizhou Zhu, Yuntao Chen, Hao Tian, Chenxin Tao, Weijie Su, Chenyu Yang, Gao Huang, Bin Li, Lewei Lu, Xiaogang Wang, et al. Ghost in the minecraft: Generally capable agents for open-world environments via large language models with text-based knowledge and memory. *arXiv preprint arXiv:2305.17144*, 2023.

[57] Shengchao Zhou, Weizhou Liu, Chen Hu, Shuchang Zhou, and Chao Ma. Unidistill: A universal cross-modality knowledge distillation framework for 3d object detection in bird's-eye view. In *Proceedings of the IEEE/CVF Conference on Computer Vision and Pattern Recognition (CVPR)*, pages 495–504, 2023.

[58] Peiyuan Zhang, Guangtao Zeng, Tianduo Wang, and Wei Lu. Tinyllama: An open-source small language model. *arXiv preprint arXiv:2401.02385*, 2024.

[59] Liyiming Ke, Yunchu Zhang, Abhay Deshpande, Siddhartha Srinivasa, and Abhishek Gupta. Ccil: Continuity-based data augmentation for corrective imitation learning. *arXiv preprint arXiv:2310.12972*, 2023.

[60] Gokul Swamy, Sanjiban Choudhury, J Bagnell, and Steven Z Wu. Sequence model imitation learning with unobserved contexts. *Advances in Neural Information Processing Systems*, 35:17665–17676, 2022.

[61] Chris Cundy and Stefano Ermon. Sequencematch: Imitation learning for autoregressive sequence modelling with backtracking. *arXiv preprint arXiv:2306.05426*, 2023.

[62] Hoang Le, Andrew Kang, Yisong Yue, and Peter Carr. Smooth imitation learning for online sequence prediction. In *International Conference on Machine Learning*, pages 680–688. PMLR, 2016.

[63] Wenyan Yang, Alexandre Angleraud, Roel S Pieters, Joni Pajarinen, and Joni-Kristian Kämäräinen. Seq2seq imitation learning for tactile feedback-based manipulation. In *2023 IEEE International Conference on Robotics and Automation (ICRA)*, pages 5829–5836. IEEE, 2023.

[64] Ruiyi Zhang, Changyou Chen, Zhe Gan, Zheng Wen, Wenlin Wang, and Lawrence Carin. Nested-wasserstein self-imitation learning for sequence generation. In *International Conference on Artificial Intelligence and Statistics*, pages 422–433. PMLR, 2020.

[65] Felipe Codevilla, Matthias Müller, Antonio López, Vladlen Koltun, and Alexey Dosovitskiy. End-to-end driving via conditional imitation learning. In *2018 IEEE international conference on robotics and automation (ICRA)*, pages 4693–4700. IEEE, 2018.

[66] Charles A Hepburn and Giovanni Montana. Model-based trajectory stitching for improved behavioural cloning and its applications. *Machine Learning*, 113(2):647–674, 2024.

[67] Mingyan Zhou, Biao Wang, and Xiatao Sun. Developing trajectory planning with behavioral cloning and proximal policy optimization for path-tracking and static obstacle nudging. *arXiv e-prints*, pages arXiv:2409, 2024.

[68] Chuan Wen, Jierui Lin, Trevor Darrell, Dinesh Jayaraman, and Yang Gao. Fighting copycat agents in behavioral cloning from observation histories. *Advances in Neural Information Processing Systems*, 33:2564–2575, 2020.

[69] Faraz Torabi, Garrett Warnell, and Peter Stone. Behavioral cloning from observation. *arXiv preprint arXiv:1805.01954*, 2018.

[70] Zachary W Robertson and Matthew R Walter. Concurrent training improves the performance of behavioral cloning from observation. *arXiv preprint arXiv:2008.01205*, 2020.

[71] Michael Janner, Yilun Du, Joshua B Tenenbaum, and Sergey Levine. Planning with diffusion for flexible behavior synthesis. *arXiv preprint arXiv:2205.09991*, 2022.

[72] Mandar Joshi, Danqi Chen, Yinhan Liu, Daniel S Weld, Luke Zettlemoyer, and Omer Levy. Spanbert: Improving pre-training by representing and predicting spans. *Transactions of the association for computational linguistics*, 8:64–77, 2020.

[73] Zi-Hang Jiang, Weihao Yu, Daquan Zhou, Yunpeng Chen, Jiashi Feng, and Shuicheng Yan. Convbert: Improving bert with span-based dynamic convolution. *Advances in Neural Information Processing Systems*, 33:12837–12848, 2020.

[74] Simon Ott, Konstantin Hebenstreit, Valentin Liévin, Christoffer Egeberg Hother, Milad Moradi, Maximilian Mayrhofer, Robert Praas, Ole Winther, and Matthias Samwald. Thoughtsource: A central hub for large language model reasoning data. *Scientific data*, 10(1):528, 2023.

[75] Mingyu Jin, Qinkai Yu, Dong Shu, Haiyan Zhao, Wenyue Hua, Yanda Meng, Yongfeng Zhang, and Mengnan Du. The impact of reasoning step length on large language models. *arXiv preprint arXiv:2401.04925*, 2024.

# Appendix

## A Structured Agent Distillation framework

### A.1 Teacher-Student Interaction Illustration

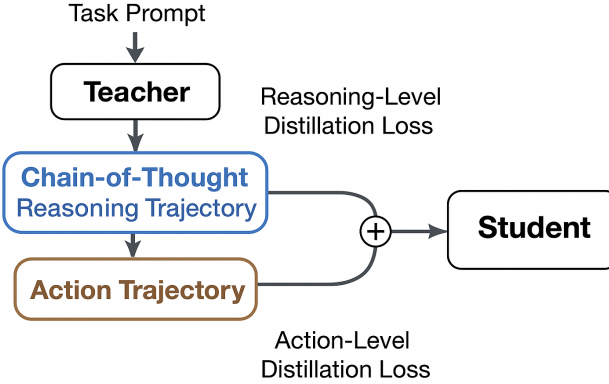


Figure 3: Illustration of the teacher-student interaction in our **Structured Agent Distillation** framework. The teacher model generates both the chain-of-thought (CoT) [74] reasoning steps and the corresponding action trajectory based on the task input. The student model learns to imitate these trajectories by minimizing both reasoning-level and action-level distillation losses. This joint supervision allows the student to capture both high-level problem-solving strategies and low-level task executions.

Figure 3 illustrates the core mechanism of our *Structured Agent Distillation* framework.

Given a task prompt, the teacher model first produces a **chain-of-thought reasoning trajectory**, which captures its intermediate thinking steps and decision rationale. It then generates an **action trajectory**, consisting of task-specific outputs (e.g., tool invocations, API calls, environment actions).

The student model receives both trajectories as supervision signals. By minimizing a combination of reasoning-level and action-level distillation losses, it learns to emulate not only the output behavior but also the underlying reasoning patterns of the teacher. This two-level guidance enables the student to generalize better across reasoning-intensive agent tasks, even with fewer parameters.

### A.2 Reasoning–Action Segmentation

To better supervise the distillation process, we segment each demonstration trajectory into two interpretable components: the **Reasoning Segment** and the **Action Segment**, as shown in Figure 4.

The **Reasoning Segment** contains the teacher’s natural language chain-of-thoughts that progressively unfold the problem-solving logic, while the **Action Segment** consists of final decisions, structured commands, or tool invocations derived from the reasoning.

During training, we apply separate segment masks  $m_r$  and  $m_a$  to isolate these parts. This enables the student model to be supervised with segment-specific objectives: a chain-of-thought imitation loss  $\mathcal{L}_{\text{cot}}$ , an action prediction loss  $\mathcal{L}_{\text{act}}$ , and a trajectory-level consistency loss  $\mathcal{L}_{\text{traj}}$ .

This design allows for fine-grained control over the learning process, encouraging the student to mimic both the rationale and the resulting behavior.

### A.3 Loss Flow in Structured Agent Distillation

Figure 5 illustrates how different loss components are computed and used to optimize the student model. The input to the student model is a trajectory consisting of both reasoning and action segments generated by the teacher model. Segment masks are applied to distinguish the two parts.

Two types of loss are computed:

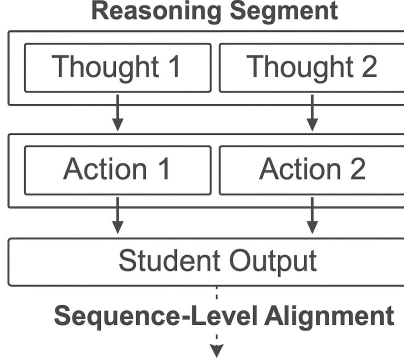


Figure 4: Illustration of the segmented trajectory structure used in our **Structured Agent Distillation** framework. The teacher’s trajectory is divided into a reasoning segment (language-based, multi-step inference) and an action segment (tool invocation or final structured decision). Each segment is used to compute a dedicated imitation loss for the student model.

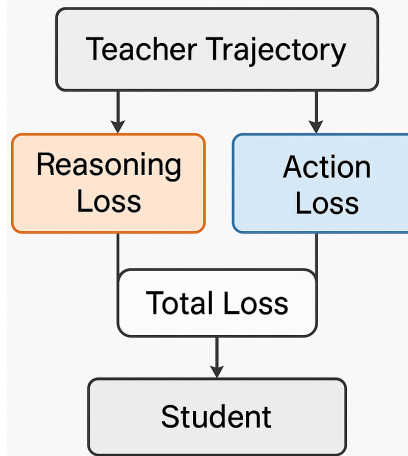


Figure 5: An overview of the loss flow in our **Structured Agent Distillation** framework. The student model learns from the teacher’s trajectory by decomposing the learning signals into reasoning and action objectives. These loss terms are aggregated to guide effective student optimization.

- **Reasoning Loss**  $\mathcal{L}_{\text{cot}}$ : aligns the student’s chain-of-thought outputs with the teacher’s intermediate reasoning steps.
- **Action Loss**  $\mathcal{L}_{\text{act}}$ : ensures that the student reproduces the teacher’s final decision or action.

These loss terms are weighted and aggregated as:

$$\mathcal{L}_{\text{total}} = \lambda_1 \mathcal{L}_{\text{cot}} + \lambda_2 \mathcal{L}_{\text{act}}$$

which is then used for backpropagation to update the student model parameters.

#### A.4 Curriculum Sampling Process

To guide the student model’s learning in a progressive manner, we apply a curriculum learning strategy. The curriculum scheduler  $\mathcal{C}$  starts with easier reasoning-action trajectories and gradually introduces harder samples as training progresses. This improves training stability and enhances generalization, especially in long-horizon tasks.

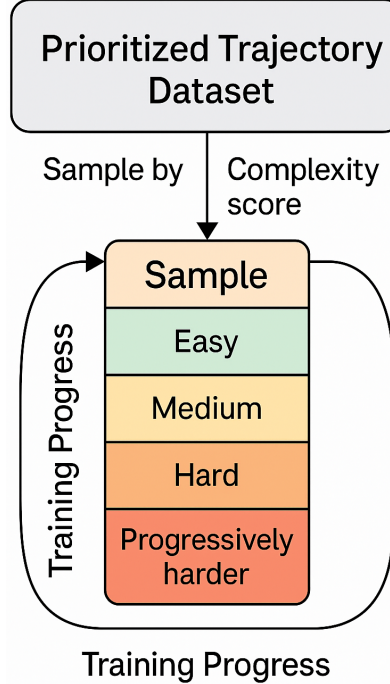


Figure 6: Illustration of the curriculum sampling process. The scheduler gradually increases task difficulty during training, guiding the student model from simple to complex **structured agent trajectories** under **Structured Agent Distillation**.

## B Task and Environment Setup

**ALFWorld.** ALFWorld [22] is an embodied instruction-following environment where agents must complete household tasks through navigation and object manipulation. Each episode provides a natural language goal (e.g., "Put the soap on the sink"), and the agent interacts with a simulated environment to achieve it. We collect teacher trajectories from a ReAct-style agent that interleaves reasoning and actions, and segment them into reasoning spans and action spans.

**WebShop.** WebShop [23] is a text-based e-commerce environment where agents must fulfill shopping goals through search, click, and buy tool invocations. Teacher agents generate structured trajectories consisting of reasoning steps (e.g., product comparisons) and concrete tool actions. Students are trained on these structured trajectories under curriculum sampling.

**HotPotQA-ReAct.** We adapt HotPotQA [1] into a ReAct-style question answering setup, where teacher agents interleave multi-hop reasoning steps before final answers. Trajectories are segmented into reasoning and action spans, ensuring a clear separation between intermediate thoughts and conclusive outputs. Students are trained to imitate these structured trajectories under segment-aware supervision.

**Training Details** All student agents are initialized for ALFWorld and WebShop. The models are fine-tuned on the collected teacher trajectories using the AdamW optimizer with the following settings:

- **Batch size:** 64 for GPT-2
- **Learning rate:**  $2 \times 10^{-5}$  with linear warmup and cosine decay
- **Max steps:** 20k steps for ALFWorld, 10k for WebShop
- **Gradient clipping:** 1.0
- **Sequence length:** 512 tokens (truncated if longer)
- **Distillation loss:** Cross-entropy for token-level, segment-aware alignment loss for our method, with optional trajectory-level contrastive term (weight  $\lambda = 0.3$ )

All models are trained on A6000 GPU, and evaluation is conducted using deterministic greedy decoding unless otherwise noted.

## C Evaluation Metrics

We evaluate models along three axes:

- **Task Success Rate (TSR) [24]:** Measures the success ratio of tasks completed by the agent:

$$\text{TSR} = \frac{N_{\text{successful tasks}}}{N_{\text{total tasks}}} \times 100\% \quad (8)$$

where  $N_{\text{successful tasks}}$  is the number of tasks where the final environment state satisfies the success conditions.

- **Reasoning Efficiency (Average Reasoning Length).** We compute the average number of tokens generated in the reasoning span of each agent trajectory. Formally, for a set of  $N$  trajectories  $\{\tau^{(i)}\}_{i=1}^N$ , the average reasoning length (ARL) is defined as:

$$\text{ARL} = \frac{1}{N} \sum_{i=1}^N \text{Length}(\tau^{(r,i)}), \quad (9)$$

where  $\tau^{(r,i)}$  denotes the reasoning span of trajectory  $\tau^{(i)}$ . This metric captures the planning efficiency of student agents, with shorter reasoning spans indicating more concise decision-making.

For instance, given three trajectories with reasoning spans of 12, 15, and 14 tokens respectively, the average reasoning length is:

$$\text{ARL} = \frac{12 + 15 + 14}{3} = 13.67. \quad (10)$$

- **Chain-of-Thought (CoT) Consistency(CoT Match Rate)** We evaluate how faithfully the student reproduces the teacher’s reasoning trace. Specifically, we compute the token-level overlap between the student’s generated reasoning span  $\tau_S^{(r,i)}$  and the teacher’s reasoning span  $\tau_T^{(r,i)}$ , and define CoT match rate as:

$$\text{CoT Match Rate} = \frac{1}{N} \sum_{i=1}^N \frac{|\tau_S^{(r,i)} \cap \tau_T^{(r,i)}|}{|\tau_T^{(r,i)}|},$$

where  $\cap$  denotes token-level intersection. Higher CoT match rates indicate better structural fidelity in reasoning reconstruction.

For instance, if a teacher reasoning span contains 9 tokens and a student’s reasoning span overlaps with 6 of them, the CoT match rate for that trajectory is:

$$\text{CoT Match Rate} = \frac{6}{9} = 66.67\%.$$

- **Latency Results (Average Reasoning Steps) [75].** As a proxy for agent latency, we measure the average number of generation steps required to complete the reasoning and action phases. Given  $N$  trajectories:

$$\text{Average Steps} = \frac{1}{N} \sum_{i=1}^N \text{Steps}(\tau^{(i)}), \quad (11)$$

where  $\text{Steps}(\tau^{(i)})$  counts the total number of generation steps (tokens or API calls) in trajectory  $\tau^{(i)}$ . Lower average steps correspond to faster decision-making and reduced i

For instance, given three sampled trajectories with total generation steps of 16, 13, and 20 respectively, the average number of steps is:

$$\text{Average Steps} = \frac{16 + 13 + 20}{3} = 16.33.$$

## D Data Construction for Structured Agent Distillation

### D.1 Trajectory Segmentation

To support **Structured Agent Distillation**, we decompose each teacher trajectory  $\tau$  into two disjoint spans: a reasoning segment  $\tau^{(r)}$  and an action segment  $\tau^{(a)}$ . This decomposition enables span-specific supervision over the student model’s reasoning and decision behaviors. Segmentation is performed using lightweight rule-based parsing tailored to each environment. Specifically:

- For **ALFWorld** and **WebShop**, each trajectory alternates between lines prefixed with `Reasoning:` and `Action:`. We extract all lines beginning with `Reasoning:` as the reasoning span  $\tau^{(r)}$ , and lines beginning with `Action:` as the action span  $\tau^{(a)}$ .
- For **HotPotQA-ReAct**, we adopt a two-phase segmentation: text preceding the final `Answer:` line is assigned to the reasoning span  $\tau^{(r)}$ , and the `Answer:` line itself is treated as the action span  $\tau^{(a)}$ .

The segmentation rules across all environments are summarized in Table 6.

Table 6: Segmentation rules for splitting teacher trajectories into reasoning and action spans.

Environment	Reasoning Span	Action Span
ALFWorld	Lines starting with <code>Reasoning:</code>	Lines starting with <code>Action:</code>
WebShop	Lines starting with <code>Reasoning:</code>	Lines starting with <code>Action:</code>
HotPotQA-ReAct	Lines starting with <code>Reasoning:</code>	Final <code>Answer:</code> line

We implement this segmentation using simple regular-expression-based pattern matching. For instance, the following patterns are used:

```
REASONING_REGEX = r"~Reasoning:\s*(.+)~"
ACTION_REGEX    = r"~Action:\s*(.+)~"
ANSWER_REGEX    = r"~Answer:\s*(.+)~" % for HotPotQA only
```

We concatenate all lines matching `Reasoning:` as the reasoning span  $\tau^{(r)}$ , and all `Action:/Answer:` lines as the action span  $\tau^{(a)}$ . This rule-based segmentation is high-precision and requires no manual annotation.

### D.2 Segment-Aware Token Mask Construction

After segmenting each trajectory into reasoning and action spans, we construct binary token-level masks to enable selective supervision during **Structured Agent Distillation**.

Let  $x_{1:T}$  denote the tokenized trajectory.

We generate two binary masks:

- Reasoning mask  $m_r(t) \in \{0, 1\}$ , where

$$m_r(t) = \begin{cases} 1 & \text{if token } x_t \text{ belongs to a reasoning span,} \\ 0 & \text{otherwise.} \end{cases}$$

- Action mask  $m_a(t) \in \{0, 1\}$ , where

$$m_a(t) = \begin{cases} 1 & \text{if token } x_t \text{ belongs to an action span,} \\ 0 & \text{otherwise.} \end{cases}$$

Each token belongs to at most one span, ensuring:

$$m_r(t) + m_a(t) \leq 1, \quad \forall t \in [1, T].$$

Tokens outside any supervised span (e.g., prompt headers, formatting artifacts) are excluded from loss computation by masking out their contributions.

**Implementation Note.** We first align the raw text spans to character offsets, then map these to token indices after tokenization. During training, the distillation losses are selectively applied over tokens using  $m_r(t)$  and  $m_a(t)$  as weights.

### D.3 Example and Loss Application

We illustrate the full segmentation and mask construction process with a concrete example.

**Input Example.** Consider a teacher-generated trajectory excerpt:

Reasoning: I should find the fridge. It's likely in the kitchen.

Action: goto kitchen

**Tokenization and Span Mapping.** After tokenizing the full sequence (e.g., using the student tokenizer), the token sequence may resemble:

$x = [\text{Reasoning}, :, \text{I}, \text{should}, \text{find}, \text{the}, \text{fridge}, ., \text{It}, ', \text{likely}, \text{in}, \text{the}, \text{kitchen}, ., \text{Action}, :, \text{goto}, \text{kitchen}]$

Based on the span segmentation, we assign masks as follows:

$$m_r = [1, 1, 1, 1, 1, 1, 1, 1, 1, 1, 1, 1, 1, 1, 0, 0, 0, 0]$$

$$m_a = [0, 0, 0, 0, 0, 0, 0, 0, 0, 0, 0, 0, 0, 0, 1, 1, 1, 1]$$

**Loss Computation.** During distillation, we apply span-specific losses weighted by these masks.

When using token-level KL divergence loss:

$$\mathcal{L}_{\text{total}} = \underbrace{\lambda_{\text{cot}} \sum_{t=1}^T m_r(t) \cdot \text{KL}(p_T(x_t) \| p_S(x_t))}_{\mathcal{L}_{\text{cot}}} + \underbrace{\lambda_{\text{act}} \sum_{t=1}^T m_a(t) \cdot \text{KL}(p_T(x_t) \| p_S(x_t))}_{\mathcal{L}_{\text{act}}}. \quad (12)$$

When using cross-entropy (CE) loss over hard targets:

$$\mathcal{L}_{\text{total}} = \underbrace{\lambda_{\text{cot}} \sum_{t=1}^T m_r(t) \cdot \text{CE}(x_t, \hat{x}_t)}_{\mathcal{L}_{\text{cot}}} + \underbrace{\lambda_{\text{act}} \sum_{t=1}^T m_a(t) \cdot \text{CE}(x_t, \hat{x}_t)}_{\mathcal{L}_{\text{act}}}. \quad (13)$$

where  $\hat{x}_t$  denotes the student model's prediction at position  $t$ .

This segment-aware supervision enables the student agent to imitate both the reasoning trace and the final action decision of the teacher, improving planning fidelity and execution robustness.

**Summary.** This appendix details the full data construction pipeline for **Structured Agent Distillation**. We describe how teacher trajectories are segmented into reasoning and action spans, how segment-aware token masks are assigned, and how these masks guide span-specific loss computation. This **structured agent supervision** enables fine-grained alignment between student and teacher agents, covering both intermediate reasoning and final action decisions.

## E Prompt Generation for Structured Agent Distillation

### E.1 Prompt Templates

We present the exact prompt formats used in each task during inference and teacher generation.

**ALFWorld.** You are in the [room]. You see: [objects]. What should you do next?

**WebShop.** User intent: Find a [product type] under [budget]. Available options: [list]. Which item should the user select?

**HotPotQA-ReAct.** Q: [question]

A: Let's think step by step. We show one representative prompt template per environment used for teacher trajectory generation.

**ALFWorld Prompt Example.** You are an intelligent agent operating in a simulated household environment. Goal: Put the soap on the sink.  
Reasoning: First, I should find where the soap is located. Action: navigate to the bathroom. Reasoning: Now I need to look for the soap in the bathroom. Action: pick up the soap. Reasoning: I should move to the sink area. Action: move to sink. Reasoning: Finally, I should place the soap on the sink. Action: place soap on sink.

**WebShop Prompt Example.** You are a shopping assistant on an online store. User goal: Find a waterproof digital camera under \$100.

Reasoning: First, I should search for waterproof cameras. Action: [Search] "waterproof camera". Reasoning: I need to filter for products under \$100. Action: [Click] "Price: Low to High" filter. Reasoning: This camera is waterproof and under budget. Action: [Buy] selected camera.

**HotPotQA-ReAct Prompt Example.** Q: Where was the author of The Origin of Species born? Let us think step by step.

Reasoning: Charles Darwin wrote The Origin of Species. Reasoning: Charles Darwin was born in Shrewsbury. Action: Shrewsbury

## E.2 Teacher Trajectory Collection

To supervise student agents via **Structured Agent Distillation**, we first collect high-quality teacher trajectories using GPT-2. All trajectories are generated offline before student training to avoid dependence on external API calls during optimization.

**Prompting Strategy.** We design task-specific ReAct-style prompts (Appendix E.1) to elicit trajectories that interleave structured reasoning and action steps. Each environment uses a tailored prompting template: natural language instruction prompts for ALFWorld, tool-oriented search prompts for WebShop, and multi-hop reasoning prompts for HotPotQA-ReAct. These trajectories are later used for **Structured Agent Distillation**.

**Generation Protocol.** For each task:

- We use a locally hosted GPT-2 model as the teacher, and generate structured trajectories via predefined prompt templates for **Structured Agent Distillation**.
- Sampling parameters are set to encourage deterministic, coherent outputs: `temperature=0.2, top_p=1.0`.
- We collect multiple structured trajectory samples per task instance to improve supervision robustness.

**Post-Processing.** Generated outputs are parsed and segmented into:

- **Reasoning spans:** intermediate deliberation steps (e.g., observations, comparisons, deductions).
- **Action spans:** concrete action decisions (e.g., navigation commands, API tool calls, final answers).

We apply minimal cleaning to correct minor formatting inconsistencies and ensure span separation consistency across examples.

**Caching and Usage.** The segmented trajectories are stored in serialized formats (e.g., JSONL) and loaded during student training. During **Structured Agent Distillation**, student models minimize reasoning and action alignment losses against these cached teacher traces without requiring real-time teacher inference.

## F Validation of Segment-Aware Mask Construction

To ensure that the reasoning and action token masks used in our **structured agent distillation loss** are accurately aligned with the intended segments, we perform two types of diagnostic validation:

### F.1 Mask Construction Rules

To enable span-specific supervision, we rely on rule-based segmentation as defined in Appendix D.1. We apply pre-defined regex patterns to extract reasoning and action spans, and validate the correctness of the resulting token masks  $\{m_r(t), m_a(t)\}$ .

**Tokenizer Alignment and Mask Assignment.** As part of **Structured Agent Distillation**, the full trajectory is tokenized using the student model’s tokenizer. We then record the token offset ranges of each span and construct binary masks accordingly.

- $m_r(t) = 1$  if token  $t$  falls within the reasoning span;
- $m_a(t) = 1$  if token  $t$  falls within the action span.

All other tokens are assigned 0. The sum  $m_r(t) + m_a(t)$  is guaranteed to be at most 1 for any token  $t$ , ensuring that supervision is applied exclusively over the intended regions.

**Tokenizer Consistency.** We ensure that all text is tokenized using the student model’s tokenizer (e.g., GPT 2 or LLaMA) to maintain consistency with the model input space. Special care is taken to preserve newline boundaries and token order, especially when combining multiple Reasoning: lines into a single span. In case of subword tokenization, spans are always aligned on token boundaries, and the original textual span is re-tokenized in isolation before alignment.

### F.2 Segment-Aware Mask Visualizations

**1. Mask Overlay Visualization.** We randomly sample 100 examples from each benchmark and overlay their segment masks on the original decoded sequences. For each sample, we color reasoning tokens in blue and action tokens in red. This visual inspection confirms that reasoning spans (e.g., multi-hop inferences, intermediate thoughts) and action spans (e.g., tool calls or answers) are clearly separated and align with their labeled boundaries. Figure 7 shows representative visualizations from WebShop, HotPotQA, and ALFWorld.

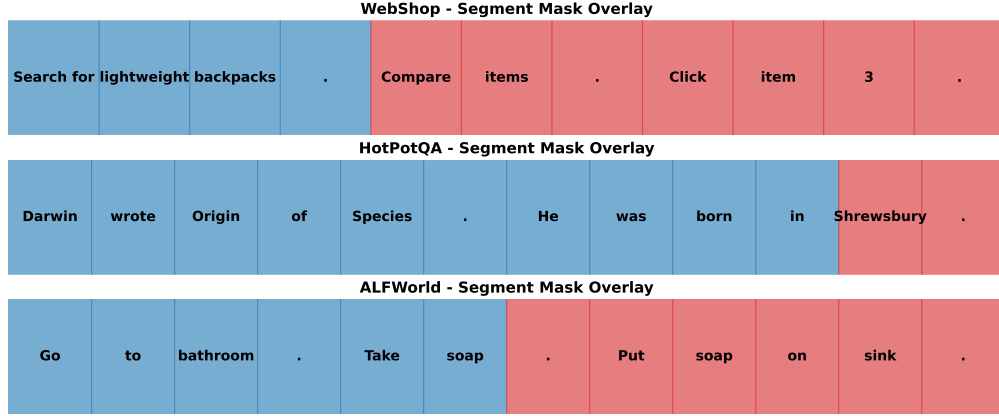


Figure 7: **Segment-Aware Token Mask Overlay across Tasks.** We visualize the token-level masks used in **Structured Agent Distillation** across three environments: WebShop, HotPotQA, and ALFWorld. Reasoning spans are shown in blue, and action spans in red. These overlays validate the alignment between the teacher’s generated structure and our mask segmentation, supporting structure-aware loss formulation.

We randomly sample 100 examples from each benchmark and overlay their segment masks on the original decoded sequences. For each sample, we color reasoning tokens in blue and action tokens in

Table 7: Task success rate (%) comparing OPT-13B and LLaMA-13B teachers, token-level baselines [9], and our **Structured Agent Distillation** students across model sizes.

Method	ALFWorld $\uparrow$	WebShop $\uparrow$	HotPotQA $\uparrow$
Teacher (OPT-13B)	76.5	73.2	82.7
Token-level-1.3B	47.8	43.2	54.1
Ours (OPT-1.3B)	<b>52.3</b>	<b>48.7</b>	<b>58.5</b>
Token-level-2.7B	55.6	51.0	62.9
Ours (OPT-2.7B)	<b>59.2</b>	<b>56.4</b>	<b>67.0</b>
Token-level-6.7B	62.8	58.6	69.7
Ours (OPT-6.7B)	<b>67.1</b>	<b>63.8</b>	<b>73.9</b>
Teacher (LLaMA-13B)	75.3	71.8	81.0
Token-level-7B	64.2	59.3	71.5
Ours (LLaMA-7B)	<b>68.0</b>	<b>64.1</b>	<b>75.2</b>

red. This visual inspection confirms that reasoning spans (e.g., multi-hop inferences, intermediate thoughts) and action spans (e.g., tool calls or answers) are clearly separated and align with their labeled boundaries. Figure 7 shows representative visualizations from WebShop, HotPotQA, and ALFWorld.

### E.3 Span Length Statistics.

To further validate the structural separation of reasoning and action segments, we compute the token length distributions of  $\tau^{(r)}$  and  $\tau^{(a)}$  across all three benchmarks. As shown in Figure 8, reasoning spans are consistently longer and more variable, reflecting multi-step deliberation processes. Action spans are shorter and more uniform, typically consisting of single answers or tool invocations. We also verify that the union of the reasoning and action masks covers 100% of the supervised tokens in all examples, with no overlaps.

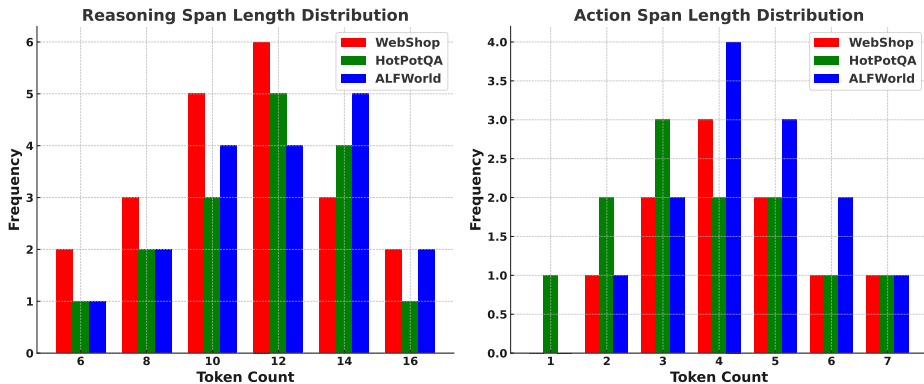


Figure 8: **Token Span Length Statistics Across Tasks.** Left: Token length distribution for reasoning spans. Right: Token length distribution for action spans. Reasoning spans tend to be longer and more variable, while action spans are concise and more consistent.

**Conclusion.** These analyses confirm that our rule-based segmentation and mask construction are robust and structurally faithful, making them suitable for **Structured Agent Distillation** without additional annotation.

Table 8: Average reasoning length (tokens) comparing OPT-13B and LLaMA-13B teachers, token-level baselines [9], and **Structured Agent Distillation** students.

Method	ALFWorld ↓	WebShop ↓	HotPotQA ↓
Teacher (OPT-13B)	38.2	35.9	40.7
Token-level-1.3B	45.7	41.8	48.5
Ours (OPT-1.3B)	<b>41.2</b>	<b>38.0</b>	<b>43.6</b>
Token-level-2.7B	42.5	39.0	45.2
Ours (OPT-2.7B)	<b>39.4</b>	<b>36.2</b>	<b>41.7</b>
Token-level-OPT-6.7B	40.8	37.2	42.9
Ours (OPT-6.7B)	<b>38.0</b>	<b>35.1</b>	<b>40.2</b>
Teacher (LLaMA-13B)	37.5	34.8	39.9
Token-level-7B	41.1	37.5	43.2
Ours (LLaMA-7B)	<b>38.2</b>	<b>34.9</b>	<b>39.8</b>

Table 9: Chain-of-Thought (CoT) match rate (%) comparing OPT-13B and LLaMA-13B teachers, token-level baselines [9], and **Structured Agent Distillation** students.

Method	ALFWorld ↑	WebShop ↑	HotPotQA ↑
Teacher (OPT-13B)	100.0	100.0	100.0
Token-level-1.3B	61.5	57.9	69.8
Ours (OPT-1.3B)	<b>67.2</b>	<b>63.8</b>	<b>74.4</b>
Token-level-2.7B	67.3	62.7	75.5
Ours (OPT-2.7B)	<b>71.6</b>	<b>67.9</b>	<b>79.8</b>
Token-level-6.7B	72.2	67.9	80.2
Ours (OPT-6.7B)	<b>76.4</b>	<b>72.5</b>	<b>84.0</b>
Teacher (LLaMA-13B)	100.0	100.0	100.0
Token-level-7B	73.0	68.3	81.2
Ours (LLaMA-7B)	<b>77.2</b>	<b>72.9</b>	<b>84.7</b>

## G Additional Experimental Results and Analysis

As shown in Figure 9, **Structured Agent Distillation** consistently outperforms token-level MinILM [9] baselines across all OPT model sizes. The gains are most pronounced for smaller models—e.g., a +4.5% improvement in task success rate at 1.3B. Our method also achieves shorter reasoning traces and higher CoT match rates, indicating better structural alignment with the teacher. Latency is consistently reduced as well, highlighting improved reasoning efficiency.

Table 10: Latency results (average steps per episode) comparing OPT-13B and LLaMA-13B teachers, token-level baselines [9], and **Structured Agent Distillation** students. Lower is better.

Method	ALFWorld ↓	WebShop ↓	HotPotQA ↓
Teacher (OPT-13B)	6.5	5.9	4.8
Token-level-1.3B	7.8	7.1	6.0
Ours (OPT-1.3B)	<b>7.0</b>	<b>6.4</b>	<b>5.3</b>
Token-level-2.7B	7.2	6.6	5.6
Ours (OPT-2.7B)	<b>6.7</b>	<b>6.1</b>	<b>5.0</b>
Token-level-6.7B	6.8	6.2	5.3
Ours (OPT-6.7B)	<b>6.5</b>	<b>5.9</b>	<b>4.9</b>
Teacher (LLaMA-13B)	6.4	5.8	4.7
Token-level-7B	6.7	6.1	5.2
Ours (LLaMA-7B)	<b>6.4</b>	<b>5.8</b>	<b>4.8</b>

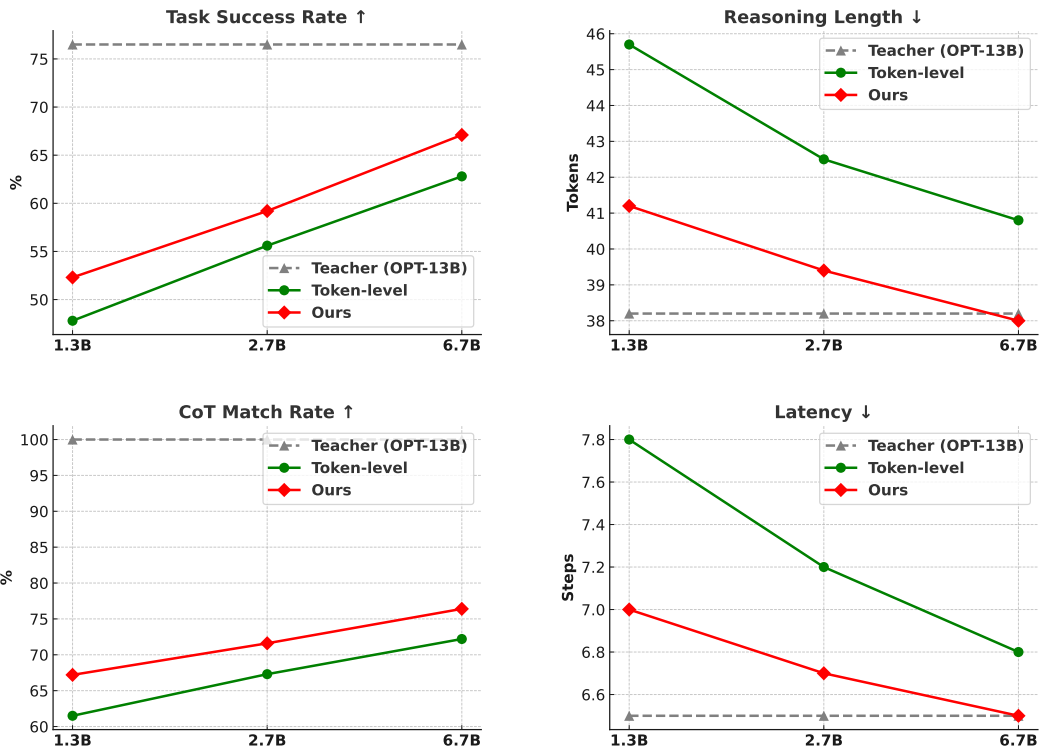


Figure 9: **Scaling analysis on OPT model family.** We compare task success rate, reasoning efficiency (avg reasoning length), CoT match rate, and latency across three OPT-based student model sizes (1.3B, 2.7B, 6.7B), using **Structured Agent Distillation** vs. token-level MiniLM [9] baselines. The OPT-13B teacher serves as a reference upper bound. **Structured Agent Distillation** consistently yields stronger performance across all metrics.